

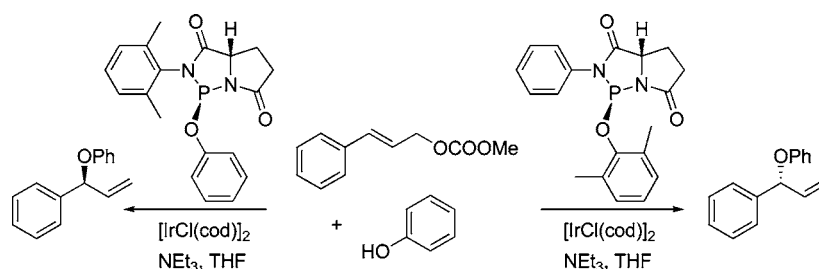
# Development of New P-Chiral Phosphorodiamidite Ligands Having a Pyrrolo[1,2-*c*]diazaphosphol-1-one Unit and Their Application to Regio- and Enantioselective Iridium-Catalyzed Allylic Etherification

Masahiro Kimura and Yasuhiro Uozumi\*

Institute for Molecular Science (IMS), CREST, and The Graduate University for Advanced Studies,  
Higashiyama 5-1, Myodaiji, Okazaki 444-8787, Japan

uo@ims.ac.jp

Received July 25, 2006



Ten types of new P-chiral phosphorodiamidite ligands having pyrrolo[1,2-*c*][1,3,2]diazaphosphol-1-one backbone were designed and prepared. They were preliminarily utilized for iridium-catalyzed asymmetric allylic etherification of cinnamyl carbonate with phenol, where both *R*- and *S*-products were obtained with good enantioselectivity (up to 74% ee) by changing the N- and P-substituents of the ligands. The opposite enantioselectivity in iridium-catalyzed allylic substitution was explained by DFT calculations of the energy difference of the  $\pi$ -allyliridium-phosphorodiamidite intermediates.

## Introduction

Asymmetric reactions catalyzed by transition metal complexes containing optically active phosphorus ligands have attracted increasing interest for their synthetic utility. One of the most exciting and challenging aspects of catalytic asymmetric synthesis is the development of chiral ligands which realize high enantioselectivity in a given reaction. Though chiral phosphine ligands having alkyl P-substituents, particularly those bearing P–P or P–N chelating functionalities, occupy a prominent position in transition metal-catalyzed asymmetric reactions, chiral phosphoramidite ligands having alkoxy and alkylamino P-substituents have recently been gaining in popularity due to their unique catalytic activity and enantiocontrolling potency. The binaphthol-based phosphoramidites **L1** (Figure 1),<sup>1</sup> originally developed by Feringa and co-workers, are representative of these compounds which have shown excellent enantioselectivity in a variety of transition metal-catalyzed asymmetric processes.<sup>2–4</sup> However, compared to the rapid and successful growth of chiral phosphoramidite ligands (P(OR)(OR′)(amino)),

only scant attention has been paid to chiral phosphorodiamidite ligands (P(OR)(amino)(amino′)). Thus, to the best of our

(2) For examples of Rh-catalyzed hydrogenation, see: (a) Peña, D.; Minnaard, A. J.; de Vries, J. G.; Feringa, B. L. *J. Am. Chem. Soc.* **2002**, *124*, 14552. (b) van den Berg, M.; Minnaard, A. J.; Haak, R. M.; Leeman, M.; Schudde, E. P.; Meetsma, A.; Feringa, B. L.; de Vries, A. H. M.; Maljaars, C. E. P.; Willans, C. E.; Hyett, D.; Boogers, J. A. F.; Henderickx, H. J. W.; de Vries, J. G. *Adv. Synth. Catal.* **2003**, *345*, 308. (c) Jerphagnon, T.; Renaud, J.-L.; Bruneau, C. *Tetrahedron: Asymmetry* **2004**, *15*, 2101.

(3) For examples of Cu-catalyzed conjugate additions: (a) Feringa, B. L.; Pineschi, M.; Arnold, L. A.; Imbos, R.; de Vries, A. H. M. *Angew. Chem., Int. Ed. Engl.* **1997**, *36*, 2620. (b) Feringa, B. L. *Acc. Chem. Res.* **2000**, *33*, 346. (c) Bertozzi, F.; Crotti, P.; Macchia, F.; Pineschi, M.; Arnold, A.; Feringa, B. L. *Org. Lett.* **2000**, *2*, 933. (d) Alexakis, A.; Trevitt, G. P.; Bernardinelli, G. *J. Am. Chem. Soc.* **2001**, *123*, 4358. (e) Alexakis, A.; Benhaim, C.; Rosset, S.; Humam, M. *J. Am. Chem. Soc.* **2002**, *124*, 5262. (f) Arnold, L. A.; Naasz, R.; Minnaard, A. J.; Feringa, B. L. *J. Org. Chem.* **2002**, *67*, 7244. (g) Watanabe, T.; Knöpfel, T. F.; Carreira, E. M. *Org. Lett.* **2003**, *5*, 4557. (h) Pineschi, M.; Del Moro, F.; Crotti, P.; Di, Bussolo, V.; Macchia, F. *J. Org. Chem.* **2004**, *69*, 2099. (i) Duursma, A.; Boiteau, J.-G.; Lefort, L.; Boogers, J. A. F.; de Vries, A. H. M.; de Vries, J. G.; Minnaard, A. J.; Feringa, B. L. *J. Org. Chem.* **2004**, *69*, 8045. (j) Suárez, R. M.; Peña, D.; Minnaard, A. J.; Feringa, B. L. *Org. Biomol. Chem.* **2005**, *3*, 729. (k) Sebesta, R.; Pizzuti, M. G.; Boersma, A. J.; Minnaard, A. J.; Feringa, B. L. *Chem. Commun.* **2005**, 1711. (l) d’Augustin, M.; Palais, L.; Alexakis, A. *Angew. Chem., Int. Ed.* **2005**, *44*, 1376. (m) Alexakis, A.; Albrow, V.; Biswas, K.; d’Augustin, M.; Prieto, O.; Woodward, S. *Chem. Commun.* **2005**, 2843.

(1) (a) Hulst, R.; de Vries, N. K.; Feringa, B. L. *Tetrahedron: Asymmetry* **1994**, *5*, 699. (b) de Vries, A. H. M.; Meetsma, A.; Feringa, B. L. *Angew. Chem., Int. Ed. Engl.* **1996**, *35*, 2374.

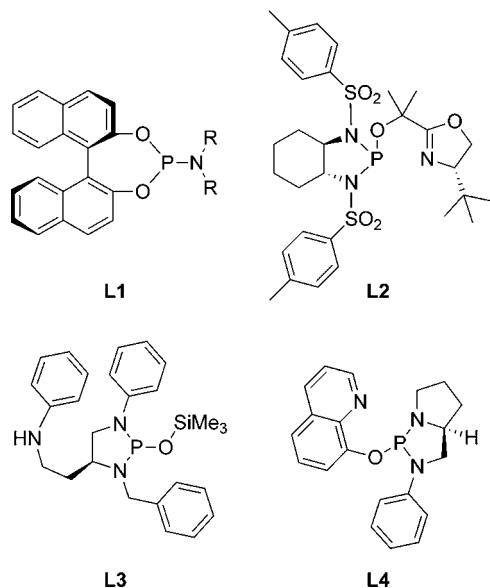
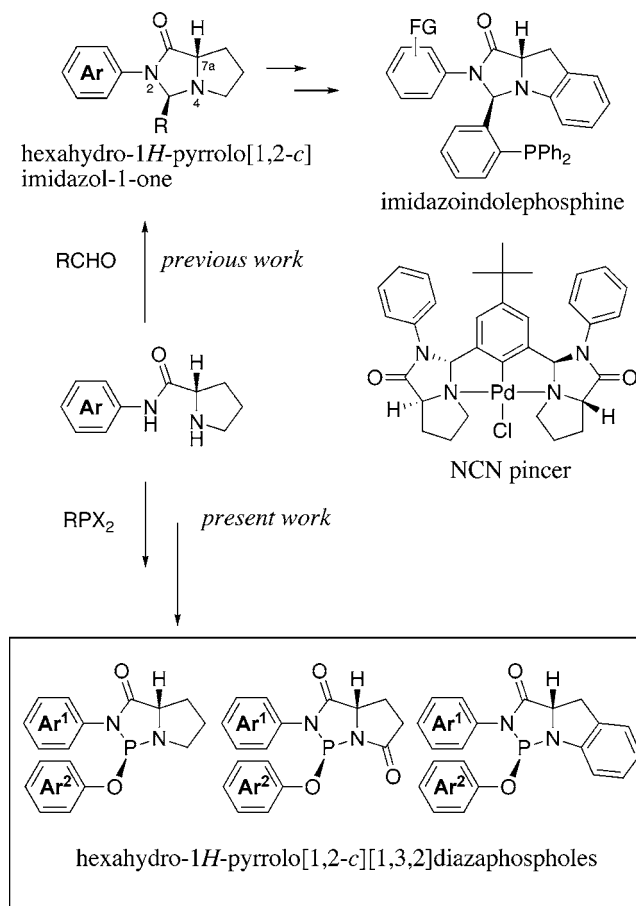


**FIGURE 1.** Chiral phosphoramidite and phosphorodiamidite ligands.

knowledge, only three types of chiral diamine-based phosphorodiamidite ligands exhibiting good to excellent enantioselectivity have been developed so far, **L2**, **L3**, and **L4** (Figure 1).<sup>5–7</sup>

During our studies on the development of powerful chiral agents, a hexahydro-1*H*-pyrrolo[1,2-*c*]imidazolone framework bearing a bicyclic [3.3.0] backbone with an *N*-chiral bridgehead nitrogen atom was identified as a highly stereoselective chiral unit. Readily prepared from proline anilides,<sup>8</sup> it was used to prepare the imidazoindolephosphine ligand<sup>9</sup> and the NCN pincer palladium complex.<sup>10</sup> As part of our ongoing effort to develop wide utility for this chiral unit, we decided to replace the skeletal carbon atom with a coordinating phosphorus atom to construct chiral phosphorodiamidite ligands bearing the hexahydro-1*H*-pyrrolo[1,2-*c*][1,3,2]diazaphosphole backbone (Scheme 1). Herein

**SCHEME 1**



we describe the design and preparation of the chiral phosphorodiamidite ligands and their preliminary use in Ir-catalyzed asymmetric allylic etherification.

## Results and Discussion

**Preparation of Phosphorodiamidite Ligands.** Phosphorodiamidite ligands having the *N*-phenyl-*P*-phenoxy substituents (**3*R*,7*a*S**)-**1a**, (**3*R*,7*a*S**)-**1b**, and (**3*R*,7*a*S**)-**1c** were readily prepared by the reaction of phenylphosphorodichloridite with anilides of (*S*)-proline (**2**), (*S*)-pyroglutamic acid (**3**), and (*S*)-indoline carboxylic acid (**7**) in 65%, 76%, and 94% yield, respectively (Scheme 2 and Figure 2). Phosphorus NMR studies revealed that the phosphorodiamidites **1a–c** were obtained with almost perfect diastereoselectivities (**1a**: (**3*R*,7*a*S**)/(**3*S*,7*a*S**) = 100/0, **1b**: (**3*R*,7*a*S**)/(**3*S*,7*a*S**) = 100/0, **1c**: (**3*R*,7*a*S**)/(**3*S*,7*a*S**) = 98/2). The phosphorodiamidite ligands (**3*R*,7*a*S**)-**1d**, (**3*R*,7*a*S**)-**1e**, (**3*R*,7*a*S**)-**1f**, and (**3*R*,9*a*S**)-**1g** bearing substituted *N*-aryl groups were prepared from the corresponding substituted anilides **4**, **5**, **6**, and **8** in 82% (diastereomeric ratio (dr) = 95/5), 63% (dr = 99/1), 76% (dr = 100/0), and quantitative yield (dr = 100/0), respectively. 2,6-Disubstituted aryloxy groups were introduced onto the phosphorus atom via the triaminophosphine intermediates **9** or **10** (Scheme 3). Thus, the pyroglutamic anilide **3** and the indoline carboxylic anilide **7** reacted with tris(dimethylamino)phosphine in refluxing toluene for 12 h to give the triaminophosphines **9** and **10**, respectively. The triaminophosphines were subsequently treated with 2,6-dimethyl- or 2,6-bis(isopropyl)phenol to afford single diastereomers of (**3*R*,7*a*S**)-**1h**, (**3*R*,7*a*S**)-**1i**, and (**3*R*,9*a*S**)-**1j** in 53%, 31%, and 43% yield.

(4) For example of Ni-catalyzed hydrovinylation: Franco, G.; Faraone, F.; Leitner, W. *J. Am. Chem. Soc.* **2002**, *124*, 736.

(5) (a) Hilgraf, R.; Pfaltz, A. *Synlett* **1999**, 1814. (b) Hilgraf, R.; Pfaltz, A. *Adv. Synth. Catal.* **2005**, *347*, 61.

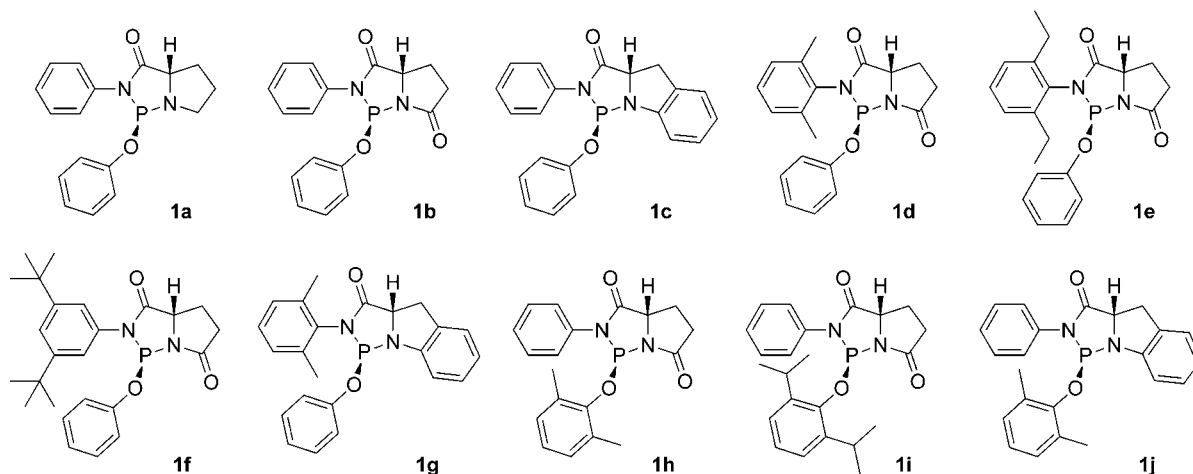
(6) (a) Nemoto, T.; Matsumoto, T.; Masuda, T.; Hitomi, T.; Hatano, K.; Hamada, Y. *J. Am. Chem. Soc.* **2004**, *126*, 3690. (b) Nemoto, T.; Masuda, T.; Matsumoto, T.; Hamada, Y. *J. Org. Chem.* **2005**, *70*, 7172.

(7) For asymmetric reactions by use of ligand **L4**, see: (a) Brunel, J. M.; Constantieux, T.; Labande, A.; Lubatti, F.; Buono, G. *Tetrahedron Lett.* **1997**, *38*, 5971. (b) Muchow, G.; Burnel, J. M.; Maffei, M.; Pardigon, O.; Buono, G. *Tetrahedron* **1998**, *54*, 10435. (c) Burnel, J. M.; Campo, B. D.; Buono, G. *Tetrahedron Lett.* **1998**, *39*, 9663. (d) Constantieux, T.; Burnel, J. M.; Labande, A.; Buono, G. *Synlett* **1998**, 49. (e) Delapierre, G.; Constantieux, T.; Burnel, J. M.; Buono, G. *Eur. J. Org. Chem.* **2000**, 2507. (f) Burnel, J. M.; Tenaglia, A.; Buono, G. *Tetrahedron: Asymmetry* **2000**, *11*, 3585. (g) Ansell, J.; Wills, M. *Chem. Soc. Rev.* **2002**, *31*, 259. (h) Gavrilov, K. N.; Tsarev, V. N.; Shiryayev, A. A.; Bondarev, O. G.; Lyubimov, S. E.; Benetsky, E. B.; Korlyukov, A. A.; Antipin, M. Y.; Davankov, V. A.; Gais, H.-J. *Eur. J. Org. Chem.* **2004**, 629. (j) Tsarev, V. N.; Lyubimov, S. E.; Shiryayev, A. A.; Zhiglov, S. V.; Bondarev, O. G.; Davankov, V. A.; Kabro, A. A.; Moiseev, S. K.; Kalinin, V. N.; Gavrilov, K. N. *Eur. J. Inorg. Chem.* **2004**, 2214.

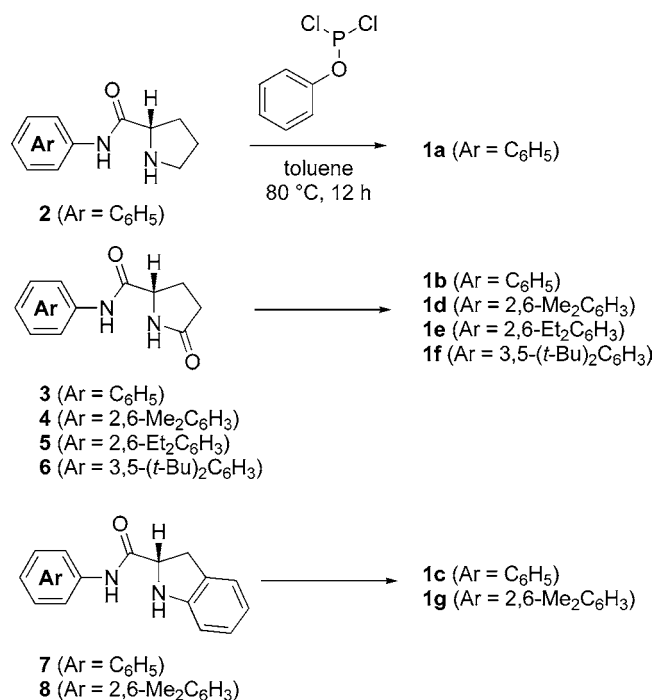
(8) (a) Uozumi, Y.; Mizutani, K.; Nagai, S.-I. *Tetrahedron Lett.* **2001**, *42*, 407. (b) Uozumi, Y.; Yasoshima, K.; Miyachi, T.; Nagai, S.-I. *Tetrahedron Lett.* **2001**, *42*, 411.

(9) (a) Uozumi, Y.; Shibatomi, K. *J. Am. Chem. Soc.* **2001**, *123*, 2919. (b) Shibatomi, K.; Uozumi, Y. *Tetrahedron: Asymmetry* **2002**, *13*, 1769. (c) Uozumi, Y.; Tanaka, H.; Shibatomi, K. *Org. Lett.* **2004**, *6*, 281. (d) Nakai, Y.; Uozumi, Y. *Org. Lett.* **2005**, *7*, 291. (e) Uozumi, Y.; Kimura, M. *Tetrahedron: Asymmetry* **2006**, *17*, 161.

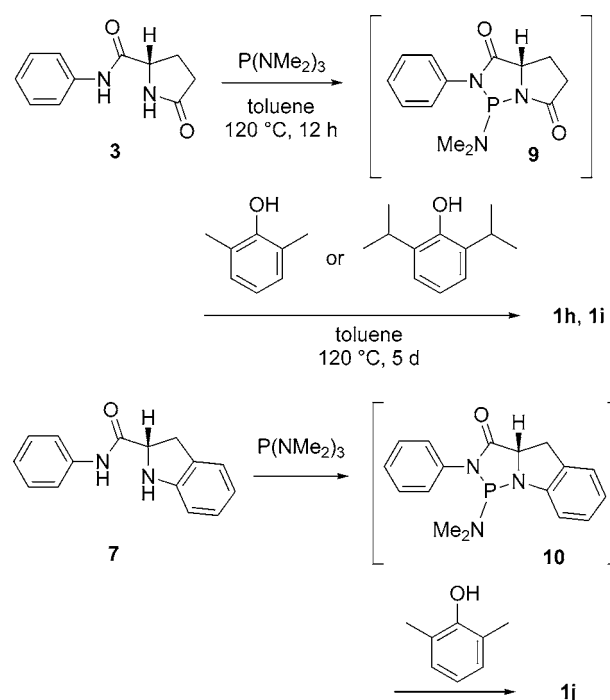
(10) (a) Takenaka, K.; Uozumi, Y. *Org. Lett.* **2004**, *6*, 1833. (b) Takenaka, K.; Uozumi, Y. *Adv. Synth. Catal.* **2004**, *346*, 1693. (c) Takenaka, K.; Minakawa, M.; Uozumi, Y. *J. Am. Chem. Soc.* **2005**, *127*, 12273.

FIGURE 2. Chiral phosphorodiamidite ligands **1a–j**.

## SCHEME 2



## SCHEME 3



All phosphorodiamidites **1a–j** were isolated by chromatography on silica gel and the diastereomeric ratios were determined by  $^{31}\text{P}\{^1\text{H}\}$  NMR and GC experiments.

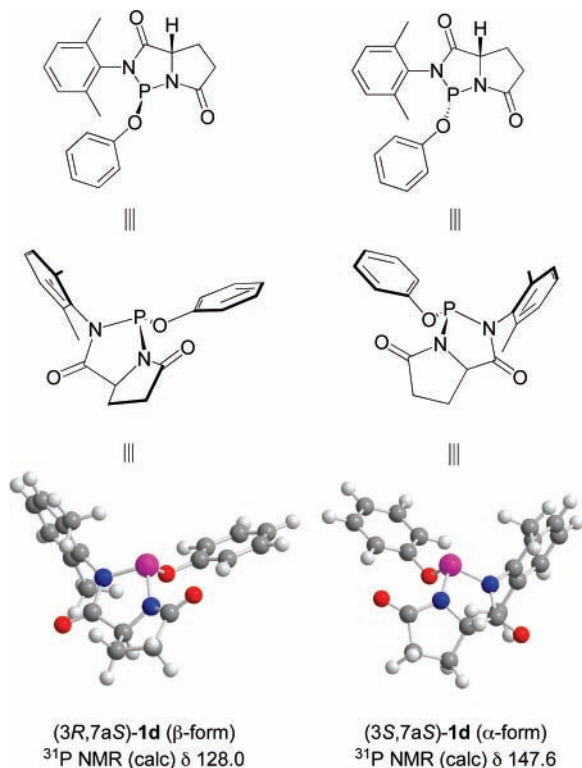
**Structural Studies.** Since the stereochemical structures of the major diastereomers of **1a–j** could not be determined by X-ray diffraction because of the difficulty in obtaining an adequate single-crystal suitable for X-ray diffraction studies, or spectroscopic studies (e.g., NOE experiments), we therefore examined DFT calculations of the relative energies of each set of  $\beta$ - and  $\alpha$ -isomers of **1a–j** (Table 1). The geometry optimizations of all  $\beta$ - and  $\alpha$ -isomers were carried out at the B3LYP/6-31G(d) level. The relative energies of all  $\beta$ -isomers (*R*-configuration) were ascertained to be 2.15–3.83 kcal/mol lower than the corresponding  $\alpha$ -isomers, as shown in Table 1. The DFT calculated NMR simulations of the  $^{31}\text{P}$  resonance were also examined for compound ( $3R^*$ ,  $7aS^*$ )-**1d** and its  $\alpha$ -isomer ( $3S^*$ ,  $7aS$ )-**1d** by the Gauge-Independent Atomic Orbital method<sup>11</sup> (GIAO-B3LYP) with basis sets 6-311G(3d) for the phosphorus atom and 6-311G(d) for the other atoms in their optimized

TABLE 1. Yield, Diastereomeric Ratio, and Calculated Relative Energy of Ligand **1a–j**

entry	ligand	yield (%) <sup>a</sup>	dr <sup>b</sup>	$\Delta E$ ( $\beta$ - $\alpha$ ) (kcal/mol) <sup>c</sup>
1	<b>1a</b>	65	100/0	-2.88
2	<b>1b</b>	76	100/0	-2.58
3	<b>1c</b>	94	98/2	-2.64
4	<b>1d</b>	82	95/5	-2.45
5	<b>1e</b>	63	99/1	-2.47
6	<b>1f</b>	76	100/0	-2.58
7	<b>1g</b>	quant.	100/0	-2.22
8	<b>1h</b>	53	100/0	-2.15
9	<b>1i</b>	31	100/0	-2.30
10	<b>1j</b>	43	100/0	-3.83

<sup>a</sup> Isolated yield. <sup>b</sup> Determined by  $^{31}\text{P}$  NMR. <sup>c</sup> Relative energy of  $\beta$ -form to  $\alpha$ -form calculated at the B3LYP/6-31G(d) level.

structure, obtained using the above-mentioned DFT calculations (Figure 3). The calculated phosphorus resonances ( $\delta$  values) of the  $\beta$ - and  $\alpha$ -isomers were +128.0 and +147.6 ppm, respectively, where the  $^{31}\text{P}$  NMR signal of the  $\beta$ -isomer is expected



**FIGURE 3.** Optimized structures and calculated chemical shifts of (3*R*,7*aS*)- and (3*S*,7*aS*)-**1d**. Geometry optimization was carried out at the B3LYP/6-31G(d) level. Magnetic shieldings of phosphorus were calculated by the GIAO-B3LYP method with 6-311G(3d) for P and 6-311G(d) for others on the optimized structures, which were transformed to NMR chemical shifts by the equation,  $\text{shift}(X) - \text{shift}(\text{ref}) = -\text{shield}(X) + \text{shield}(\text{ref})$ . ( $\text{shield}(\text{ref} = \text{P}(\text{OMe})_3) = 149.86$  ppm,  $\text{shift}(\text{ref} = \text{P}(\text{OMe})_3) = 140$  ppm).

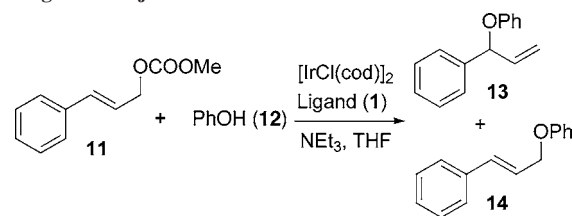
to appear at higher field with a  $\Delta\delta$  value of 19.6 ppm compared to that of the  $\alpha$ -isomer ( $\Delta\delta_{\text{calc}}(\beta - \alpha) = -19.6$ ). The  $^{31}\text{P}$  NMR chemical shifts ( $\delta$  values) of the major and the minor diastereomers of **1d** were observed at +106.6 and +124.2 ppm ( $\Delta\delta_{\text{obs}}(\beta - \alpha) = -17.6$ ), respectively, in a ratio of 95/5 to show good agreement with the results of the DFT-assisted NMR simulations. These results indicate that the major diastereomer of **1d** is the  $\beta$ -form, (3*R*\*,7*aS*)-**1d**.

The DFT calculation of the energy profile for the epimerization of P-central chirality was also examined for the ligand **1b** (Figure 4). It should be noted that ca. 97 kcal/mol of energy is required for the epimerization of P-central chirality to demonstrate the stability of P-chirality during the reaction conditions (*vide infra*).

#### Phosphorodiamidite Ligands in Asymmetric Catalysis.

The stereocontrolling potentials of the ligands **1a–j** were examined for the iridium-catalyzed asymmetric allylic etherification of cinnamyl carbonate (**11**) with phenol (**12**). Since Takeuchi's pioneering findings of Ir-catalyzed branch-selective allylic substitution of linear allylic esters in 1997,<sup>12</sup> chiral-switching of the catalysis has received much attention.<sup>13</sup> Thus, in 2003, Hartwig and co-workers applied the binaphthyl-based

**TABLE 2.** Iridium-Catalyzed Asymmetric Allylic Etherification with Ligands **1a–j**<sup>a</sup>

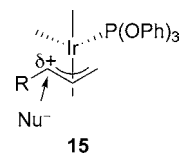


entry	ligand	yield (%) <sup>b</sup>	<b>13</b> / <b>14</b> <sup>c</sup>	ee (%) <sup>d</sup>	config
1	<b>1a</b>	8	92/8	18	<i>R</i>
2	<b>1b</b>	63	91/9	11	<i>S</i>
3	<b>1c</b>	50	87/13	70	<i>R</i>
4	<b>1d</b>	22	97/3	70	<i>S</i>
5	<b>1e</b>	54	96/4	40	<i>S</i>
6	<b>1f</b>	58	96/4	62	<i>S</i>
7	<b>1g</b>	30	94/6	16	<i>S</i>
8	<b>1h</b>	76	73/27	74	<i>R</i>
9	<b>1i</b>	71	31/69	5	<i>S</i>
10	<b>1j</b>	7	90/10	60	<i>R</i>

<sup>a</sup> All reactions were carried out at 50 °C for 20 h. The ratio of cinnamyl carbonate (mol)/ phenol (mol)/triethylamine (mol)/iridium (mol)/ligand (mol)/THF (L) = 1.0/2.0/2.0/ 0.02/0.02/1.0. <sup>b</sup> Isolated yields of **13** and **14**.

<sup>c</sup> Determined by  $^1\text{H}$  NMR of crude reaction mixtures. <sup>d</sup> Determined by HPLC analysis with a chiral stationary phase column (CHIRALCEL OJ-H).

#### CHART 1



chiral phosphoramidite ligand to iridium catalysis with aryl-oxides to achieve up to 97% stereoselectivity.<sup>14</sup> Our continuing interest in asymmetric allylic etherification<sup>9e</sup> led us to examine the Ir-catalyzed reaction of cinnamyl carbonate with phenol in the presence of the chiral phosphorodiamidite ligands **1**. The reaction of cinnamyl methyl carbonate (**11**) with 2 equiv of phenol (**12**) was carried out in THF at 50 °C for 20 h in the presence of 2 equiv of triethylamine and with an iridium complex generated in situ by mixing 1 mol % of bis[(1,5-cyclooctadiene)iridium(I) chloride] ( $[\text{IrCl}(\text{cod})]_2$ ) and 2 mol % of the ligand to give 1-phenyl-1-phenoxy-2-propene (**13**) and 1-phenyl-3-phenoxy-2-propene (**14**).  $^1\text{H}$  NMR of a crude reaction mixture revealed a ratio of regioisomers (**13**/**14**). Enantiomeric purity of the branched product **13** was determined by HPLC analysis with a chiral stationary phase column. The absolute configuration of **13** was determined by comparison of

(13) For asymmetric  $\pi$ -allylic alkylation with high stereoselectivity, see: (a) Alexakis, A.; Polet, D. *Org. Lett.* **2004**, *6*, 3529. (b) Lipowsky, G.; Miller, N.; Helmchen, G. *Angew. Chem., Int. Ed.* **2004**, *43*, 4595. For amination: (c) Welter, C.; Dahnz, A.; Brunner, B.; Streiff, S.; Dübon, P.; Helmchen, G. *Org. Lett.* **2005**, *7*, 1239. (d) Leitner, A.; Shu, C.; Hartwig, J. F. *Org. Lett.* **2005**, *7*, 1093. (e) Leitner, A.; Shekhar, S.; Pouy, M. J.; Hartwig, J. F. *J. Am. Chem. Soc.* **2005**, *127*, 15506. (f) Kiener, C. A.; Shu, C.; Incarvito, C.; Hartwig, J. F. *J. Am. Chem. Soc.* **2003**, *125*, 14272. (g) Ohmura, T.; Hartwig, J. F. *J. Am. Chem. Soc.* **2002**, *124*, 15164. (h) Shu, C.; Leitner, A.; Hartwig, J. F. *Angew. Chem., Int. Ed.* **2004**, *43*, 4797. (i) Tissant-Crosset, K.; Polet, D.; Alexakis, A. *Angew. Chem., Int. Ed.* **2004**, *43*, 2426.

(14) (a) López, F.; Ohmura, T.; Hartwig, J. F. *J. Am. Chem. Soc.* **2003**, *125*, 3426. (b) Kiener, C. A.; Shu, C.; Incarvito, C.; Hartwig, J. F. *J. Am. Chem. Soc.* **2003**, *125*, 14272. (c) Shu, C.; Hartwig, J. F. *Angew. Chem., Int. Ed.* **2004**, *43*, 4794. (d) Leitner, A.; Shu, C.; Hartwig, J. F. *Org. Lett.* **2005**, *7*, 1093.

(11) (a) Ditchfield, R. *Mol. Phys.* **1974**, *27*, 789. (b) Wolinski, K.; Hilton, J. F.; Pulay, P. *J. Am. Chem. Soc.* **1990**, *112*, 8251.

(12) (a) Takeuchi, R.; Kashio, M. *Angew. Chem., Int. Ed. Engl.* **1997**, *36*, 263. (b) Takeuchi, R.; Kashio, M. *J. Am. Chem. Soc.* **1998**, *120*, 8647. (c) Takeuchi, R.; Ue, N.; Tanabe, K.; Yamashita, K.; Shiga, N. *J. Am. Chem. Soc.* **2001**, *123*, 9525.



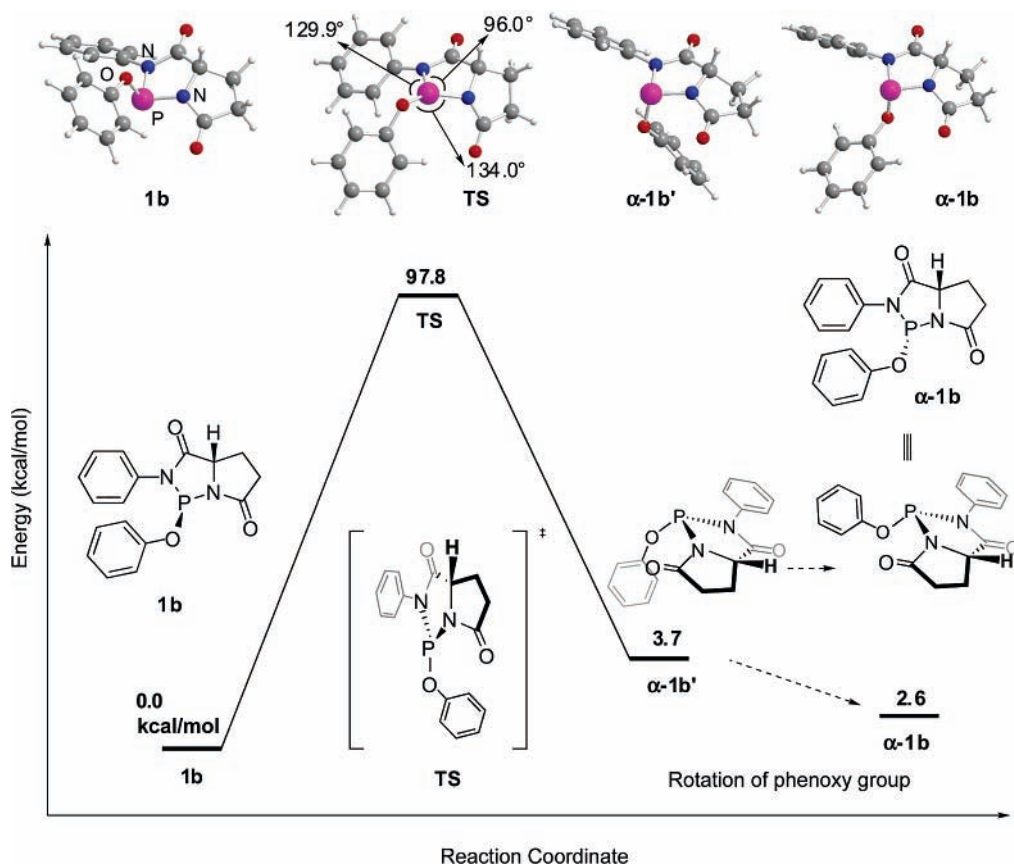


FIGURE 4. Energy profile for the epimerization of P-chirality of **1b**. Geometry optimization was carried out at the B3LYP/6-31G(d) level.

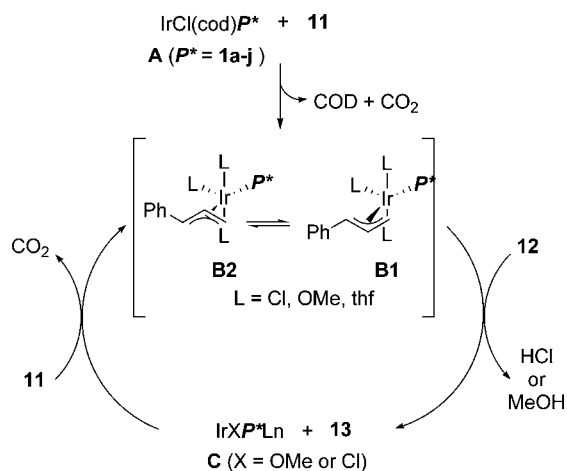
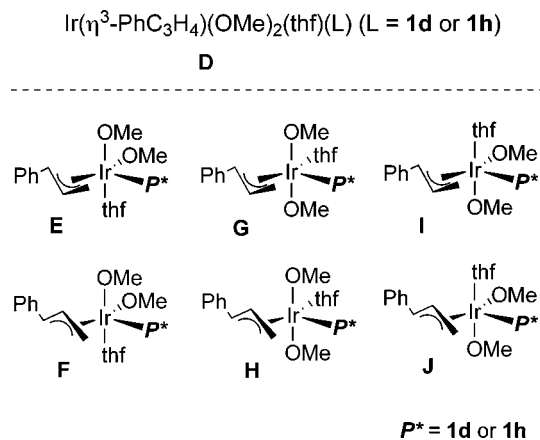


FIGURE 5. Plausible reaction pathway of the iridium-catalyzed allylic etherification of cinnamyl carbonate with phenol.

the optical rotation with (*S*)-**13** prepared by the reaction of (*R*)-1-phenyl-2-propen-1-ol with phenol under Mitsunobu conditions. Representative results are summarized in Table 2. The catalyst with the L-proline-derived ligand **1a** gave the allyl phenyl ethers **13** and **14** in only 8% yield with 18% ee (*R*) (entry 1). On the other hand, ligand **1b** gave the opposite and poor enantioselectivity (11% ee (*S*), entry 2). Ligand **1c**, which was derived from (*S*)-(-)-indoline-2-carboxylic acid, gave 70% ee of (*R*)-**13** with unsubstituted phenyl rings as both *N*-Ar and *P*-OAr groups (entry 3). Although reactivity was low (22% yield), the highest regioselectivity (**13/14** = 97/3) and good

CHART 2



enantioselectivity (70% ee (*S*)) were observed with ligand **1d** having the *N*-(2,6-dimethylphenyl) group. (entry 4). Ligands **1e** and **1f** bearing the 2,6-diethylphenyl and the 3,5-di-*tert*-butylphenyl groups as *N*-substituents provided lower enantioselectivities: 40% ee and 62% ee, respectively (entries 5 and 6). The use of the indolinecarboxylic acid-derived ligand **1g** having the *N*-(2,6-dimethylphenyl) group gave (*S*)-**13** with only 16% ee (entry 7). The best enantioselectivity was obtained when ligand **1h**, prepared from L-pyroglutamic acid, having methyl groups at the 2,6-positions of the *P*-phenoxy group was used (entry 8). The allyl ethers **13** and **14** were obtained in 76% yield with 73/27 regioselectivity and 74% ee (*R*). Ligand **1i** having bulky isopropyl groups at the 2,6-positions remarkably lowered both the regioselectivity and the enantioselectivity (**13/14** = 31/

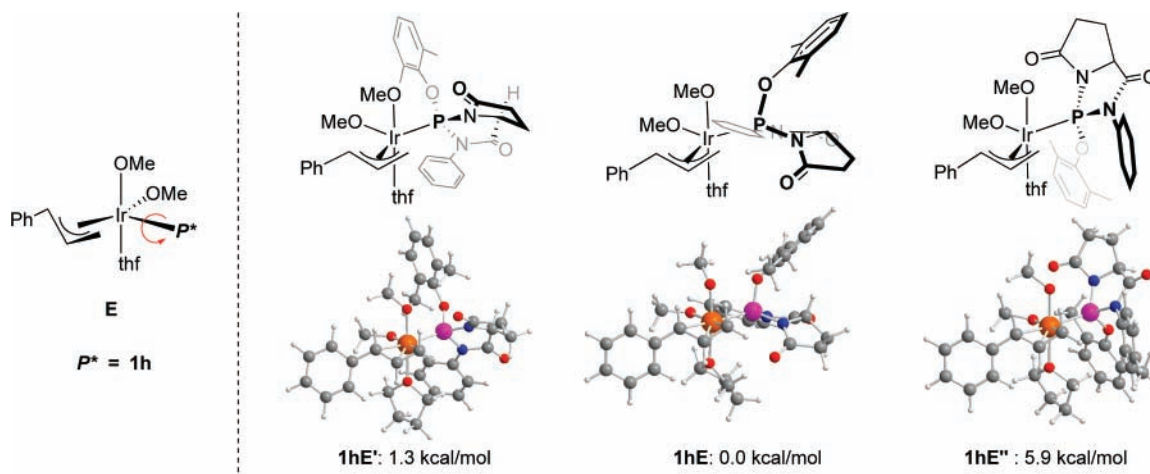


**FIGURE 6.** Optimized structures and relative energies of complex **1hE** and its isomers (**1hE'** and **1hE''**) at the B3LYP/3-21G\* (LanL2DZ for Ir) level.

69, 5% ee; entry 9). Moderate enantioselectivity (60% ee) was obtained by use of the indolinecarboxylic acid-derived ligand **1j** having 2,6-dimethyl groups on the *P*-phenoxy group (entry 10). It should be noted that the stereochemical outcome of the Ir-catalyzed allylic etherification is strongly affected by the substituents of the *N*-aryl and the *P*-aryloxy groups. Thus, the *N*-(2,6-dimethylphenyl) ligand **1d** gave (*S*)-**13** with 70% ee, whereas the *P*-(2,6-dimethylphenoxy) ligand **1h** gave 74% ee of the opposite enantiomer (*R*)-**13**, both of which were derived from the same chiral source, (*S*)-pyroglutamic acid.

**Mechanistic Discussion with DFT Calculation.** Considering the crucial role of the *N*- and *P*-substituents of the ligand in the stereodiscrimination steps, we were prompted to elucidate the reaction pathway of the present allylic substitution with the chiral phosphorodiamidite ligands. Takeuchi proposed the intermediacy of a  $\pi$ -allyliridium complex **15** to elucidate the high branch selectivity observed in his system.<sup>15</sup> Thus, triphenyl phosphite coordinates with the metal trans to the substituted allylic terminus to avoid steric repulsion, and nucleophilic substitution takes place at the relatively cationic allylic terminus to give the branched product (Chart 1).

According to Takeuchi's rationale, the reaction pathway of the present asymmetric iridium-catalyzed allylic etherification of cinnamyl carbonate with phenol would be as shown in Figure 5. The phosphorodiamidite–IrCl(cod) complex **A** generated in situ by mixing [IrCl(cod)]<sub>2</sub> and a phosphorodiamidite ligand reacts with the cinnamyl carbonate **11** to give  $\eta^3$ -(1-phenyl)propenyl iridium(III) complex **B**. Nucleophilic attack of the phenoxy anion at the substituted allylic terminus would give the desired branched product **13** and the iridium(I) complex **C** by releasing an anion X (X = Cl or OMe). Oxidative addition of cinnamyl carbonate to the complex **C** occurs again to give the  $\eta^3$ -(1-phenyl)propenyl iridium(III) complex **B**. Nucleophilic attack of phenoxy anion completes the catalytic cycle.

According to the mechanistic insight, the reaction pathways giving the opposite enantiomers with ligands **1d** and **1h** (entry 4 vs 8, Table 2) were studied by DFT calculations of the relative thermodynamic stability of the  $\eta^3$ -(1-phenyl)propenyl iridium(III) intermediate **D** [Ir(OMe)<sub>2</sub>(thf)(ligand **1d** or **1h**)].<sup>16</sup> The relative energies of the six isomers of the  $\eta^3$ -(1-phenyl)propenyl iridium(III)-phosphorodiamidites **E–J** (Chart 2) for each ligand

were calculated. The geometry optimization was performed using the B3LYP method with LanL2DZ for iridium and 3-21G\* for others as the basis sets. The phosphorodiamidite ligand was fixed trans to the substituted allylic terminus. First, the most stable configuration of the coordinated ligand was explored (by rotation of the Ir–P bond) using the complex **E**. Figures 6 and 7 show the results of the relative energies and the optimized structures for ligands **1h** and **1d**, respectively. It was found that the conformation of **1hE** makes a more stable complex than **1hE'** (1.3 kcal/mol) and **1hE''** (5.9 kcal/mol) for ligand **1h** (Figure 6). On the other hand, in the case of ligand **1d**, the conformation of the complex **1dE** was stable compared to those of **1dE'** (3.6 kcal/mol) and **1dE''** (4.7 kcal/mol), as shown in Figure 7. These results indicate that both the 2,6-dimethyl substituents on the phenoxy group in ligand **1h** and the anilino group in **1d** are located in the less hindered space (nonsubstituted allylic terminus) to avoid the steric repulsion between the bulky 2,6-dimethylphenyl group and the other ligands (OMe or THF).

The energy calculations of the possible  $\pi$ -allyliridium intermediates **1hF–hJ** and **1dF–dJ** were carried out using the configuration of the phosphorodiamidite ligand obtained in the complexes **1hE** or **1dE** for the initial structure. Figure 8 shows the optimized structures and relative energies of the complexes **1hE–hJ**, among which complex **1hH** was identified as the most stable. Thus, the  $\pi$ -allyl intermediate **1hH** giving (*R*)-**13** (Chart 3) was 3.4 kcal/mol more stable than the intermediate **1hG** resulting in the *S*-isomer (**1hG** (−7.6 kcal/mol) vs **1hH** (−11.0 kcal/mol)). The DFT-assisted stereochemical prediction showed good agreement with the enantioselectivity obtained with ligand **1h**. Similarly, the most stable  $\pi$ -allyliridium complex of the ligand **1d** was calculated to be **1dG** leading to the *S*-form **13**, the energy of which was 1.8 kcal/mol lower than that of **1dH** (Figure 9).<sup>17</sup> The simulation of ligand **1d** was also consistent with the experimental results giving (*S*)-**13** as the major enantiomer with **1d** (Chart 3).

(16) It is yet unclear if the enantioselectivity of this catalysis was controlled by the thermodynamic stabilities of the  $\pi$ -allyliridium intermediates via the  $\pi$ -allylic isomerization (B1–B2 equilibrium of Figure 5) or by the kinetic  $\pi$ -face selective oxidative addition to form  $\pi$ -allyliridium intermediates (ref 13a). The energy profiles of *R*- and *S*-selective kinetic oxidative addition should be affected by the thermodynamic stability of the products of this step, i.e.  $\pi$ -allyliridium intermediates.

(15) Takeuchi, R. *Polyhedron* **2000**, *19*, 557.

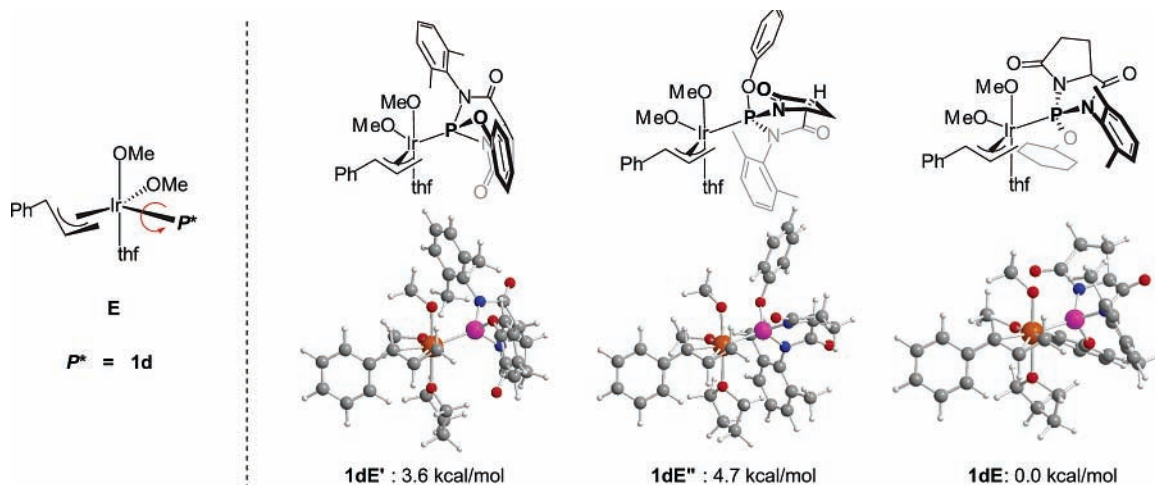


FIGURE 7. Optimized structures and relative energies of complex **1dE** and its isomers (**1dE'** and **1dE''**) at the B3LYP/3-21G\* (LanL2DZ for Ir) level.

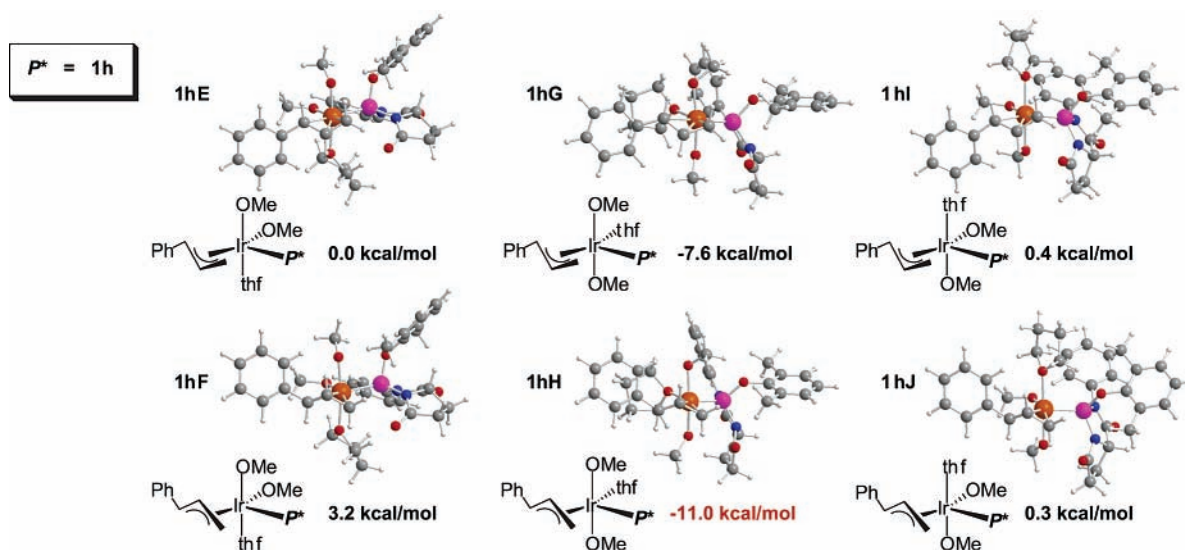
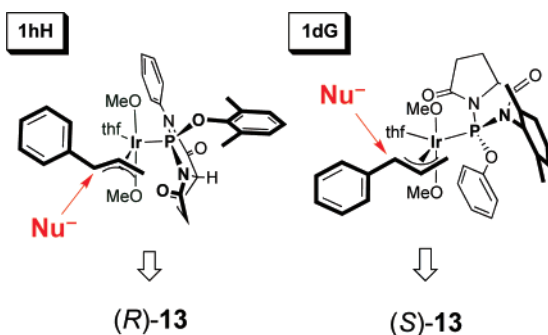


FIGURE 8. Optimized structures and relative energies of complexes **1hE–hJ** calculated at the B3LYP/3-21G\* (LanL2DZ for Ir) level.

### CHART 3



### Conclusions

In summary, we have described the development of new P-chiral phosphorodiamidite ligands having the pyrrolo[1,2-*c*]-[1,3,2]diazaphosphol-1-one unit. The ligands were utilized for iridium-catalyzed asymmetric allylic etherification of cinnamyl carbonate with phenol, where both *R*- and *S*-products were obtained with good enantioselectivity (up to 74% ee) by changing the N- and P-substituents of the ligands. Thus, (*R*)-

and (*S*)-1-phenyl-1-phenoxy-2-propenes were obtained by use of the L-pyrroglutamic acid-derived ligands **1h** and **1d**, which have *P*-(2,6-dimethylphenoxy) and *N*-(2,6-dimethylphenyl) groups, respectively. The opposite enantioselectivity in iridium-catalyzed allylic substitution was explained by DFT calculations of the energy difference of the  $\pi$ -allyliridium-phosphorodiamidite intermediates. Further fine-tuning of the N- and P-substituents thus identified effective diversity groups, and applications of the chiral phosphorodiamidite ligands for various asymmetric transformations are currently underway.

### Experimental Section

**General Procedure for the Preparation of the Phosphorodiamidite Ligand 1. Procedure A.** To a solution of the amide (1.5 mmol) and triethylamine (3.0 mmol) in toluene (15 mL) was added

(17) A referee has argued that the relationship between the thermal stabilities and the DFT-optimized structures of  $\pi$ -allyliridium complexes, e.g. **1hG**, **1hH**, **1dG**, and **1dH**, could be plausible. Thus, in the relatively stable structures **1hH** and **1dG**, the bond lengths between iridium and Ph-substituted allylic carbon were shorter than those of less stable isomeric structures, i.e. **1hG** and **1dH**. *Ir-C*(Ph)H-CHCH<sub>2</sub> (nm): **1hH** = 0.238, **1dG** = 0.243, **1hG** = 0.252, **1dH** = 0.259. We deeply appreciate the referee's suggestion.



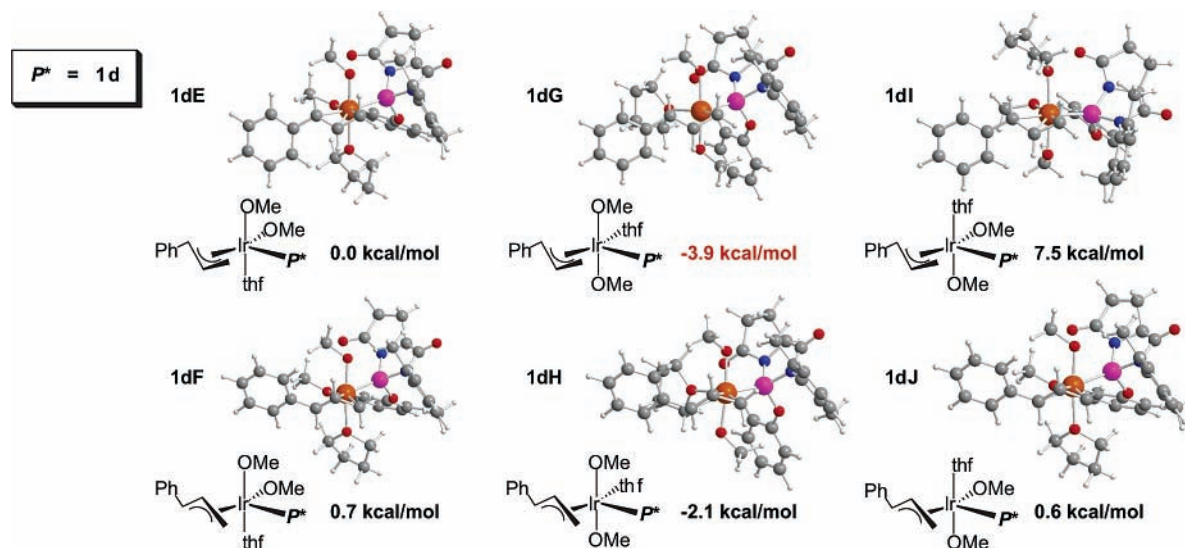


FIGURE 9. Optimized structures and relative energies of complexes **1dE**–**1dJ** calculated at the B3LYP/3-21G\* (LanL2DZ for Ir) level.

phenylphosphorodichloridite (1.5 mmol) at 0 °C. The reaction mixture was stirred at 80 °C for 12 h, and the generated triethylammonium chloride was filtered off through a dry Celite pad. The filtrate was concentrated in vacuo, and the crude products were purified by column chromatography on dry silica gel.

**Procedure B.** The mixture of the amide (1.5 mmol) and tris(dimethylamino)phosphine (1.5 mmol) in toluene (15 mL) was stirred at 120 °C for 12 h. The substituted phenol (1.5 mmol) then was added to the mixture and stirred at 120 °C for 5 days. After concentration in vacuo, the crude products were purified by column chromatography on dry silica gel.

**General Procedure for the Asymmetric Allylic Etherification of **11** with **12**.** [IrCl(cod)]<sub>2</sub> (6.7 mg, 0.01 mmol) and ligand **1** (0.02 mmol) were dissolved in THF (1.0 mL) in a sealed tube. Cinnamyl methyl carbonate (**11**, 192 mg, 1.0 mmol), phenol (**12** 188 mg, 2.0 mmol), and triethylamine (202 mg, 2.0 mmol) were successively added, and the resulting reaction mixture was stirred at 50 °C for 20 h. The reaction mixture was poured into brine and extracted with ethyl acetate. The extract was dried over Na<sub>2</sub>SO<sub>4</sub>, filtered, and concentrated in vacuo. The ratio of regioisomers **13/14** was

determined by <sup>1</sup>H NMR analysis of the crude mixture. The crude residue was purified by column chromatography on silica gel to afford the mixture of **13** and **14**. The enantiomeric excess of **13** was determined by HPLC analysis using a chiral stationary phase column (CHIRALCEL OJ-H, eluent; *n*-hexane/2-propanol = 300/1, flow rate; 0.8 mL/min, retention times; major isomer 37.9 min and minor 34.0 min).

**Calculations.** All computational calculations were carried out by using the Gaussian 98 program.<sup>18</sup> Geometries were fully optimized with Beck's three-parameter hybrid functional method (B3LYP).<sup>19</sup> Basis set LanL2DZ, which combines Hay–Wadt's effective core potential (ECP),<sup>20</sup> was used for the iridium atom in all calculations. The standard 6-31G(d) and 3-21G\* basis sets were employed for the other atoms for geometry optimization of ligands and  $\pi$ -allyliridium complexes, respectively. Magnetic shieldings were calculated by the Gauge-Independent Atomic Orbital method<sup>11</sup> (GIAO-B3LYP) on the optimized structure.

**Acknowledgment.** This work was supported by the CREST program, sponsored by the JST. We also thank the JSPS (GRANT-in-AID for Scientific Research, No.15205015) and the MEXT (Scientific Research on Priority Areas) for partial financial support of this work.

**Supporting Information Available:** Experimental details for the preparation of the amides **4**–**6** and **8** and iridium-catalyzed allylic etherification, characterization data of **1a–j**, **4**–**6**, **8**, and **13** (**14**), and <sup>1</sup>H and <sup>13</sup>C NMR charts of new compounds. Optimized structures (Cartesian coordinates) and total energies of  $\beta$ - and  $\alpha$ -**1a–j** (at B3LYP/6-31G(d) level), and iridium complexes **1hE–hJ** and **1dE–dJ** (at B3LYP/3-21G\* (LanL2DZ for Ir) level). This material is available free of charge via the Internet at <http://pubs.acs.org>.

JO0615403

(18) Gaussian 98, Revision A.9, Frisch, M. J.; Trucks, G. W.; Schlegel, H. B.; Scuseria, G. E.; Robb, M. A.; Cheeseman, J. R.; Zakrzewski, V. G.; Montgomery, J. A.; Stratmann, R. E.; Burant, J. C.; Dapprich, S.; Millam, J. M.; Daniels, A. D.; Kudin, K. N.; Strain, M. C.; Farkas, O.; Tomasi, J.; Barone, V.; Cossi, M.; Cammi, R.; Mennucci, B.; Pomelli, C.; Adamo, C.; Clifford, S.; Ochterski, J.; Petersson, G. A.; Ayala, P. Y.; Cui, Q.; Morokuma, K.; Malick, D. K.; Rabuck, A. D.; Raghavachari, K.; Foresman, J. B.; Cioslowski, J.; Ortiz, J. V.; Baboul, A. G.; Stefanov, B. B.; Liu, G.; Liashenko, A.; Piskorz, P.; Komaromi, I.; Gomperts, R.; Martin, R. L.; Fox, D. J.; Keith, T.; Al-Laham, M. A.; Peng, C. Y.; Nanayakkara, A.; Gonzalez, C.; Challacombe, M.; Gill, P. M. W.; Johnson, B.; Chen, W.; Wong, M. W.; Andres, J. L.; Gonzalez, C.; Head-Gordon, M.; Replogle, E. S.; Pople, J. A., Gaussian, Inc.: Pittsburgh, PA, 1998.

(19) (a) Lee, C.; Yang, W.; Parr, R. G. *Phys. Rev. B* **1988**, *37*, 785. (b) Becke, A. D. *J. Chem. Phys.* **1993**, *98*, 5648.

(20) Hay, P. J.; Wadt, W. R. *J. Chem. Phys.* **1985**, *82*, 299.